CHAPTER 10

SPECTRAL RESPONSE AND FLATBAND POTENTIAL MEASUREMENTS OF PEC SOLAR CELLS USING WS_xSe_{2-x} SINGLE CRYSTALS

CONTENTS

10.1 Introduction

Optical properties of the photoelectrochemical (PEC) cells not only depend on the nature of the photoelectrode but also on the characteristics of the incident light, namely wavelength and intensity. Properties of the semiconductor electrode such as band gap energy, conductivity and nature of the semiconductor surface affect these optical properties. Presence of surface states and recombination centres in the semiconductor also influence these optical properties. The impurities added deliberately or unintentionally provide recombination centres, surface states, and produce additional donor or acceptor levels, in between the conduction band and valence band. In a material like Bi_xSe_{2-x} , the conductivity and its type are determined by the defect structure of the semiconductor. The conductivity is influenced by the presence of vacancies and/or interstitials and impurity ions which provide scattering centres for the electrons. The presence of impurity ions causes a perturbation in the interaction resulting in a shift of the conduction band of the semiconductor. Therefore along with a change in the band gap energy, a change in the current efficiency of the semiconductor liquid junction cell is also observed.

The spectral sensitivity of a PEC cell is

an important parameter, because it is directly related to the solar spectrum utilization. It is investigated by taking spectral response of the grown crystals of WS_xSe_{2-x}. The direct band gaps are determined from the peak values as well as from on set values of the photocurrent spectra recorded at different wavelengths.

In order to locate the positions of conduction band, valence band and Fermi level, flat band potential is estimated from Mott-Schottky plots for the WS_xSe_{2-x} single crystals used in the PEC cells.

Thus the remaining characterization of the PEC cell by determining spectral response and flat band potential measurements is presented in this chapter.

10.2 Experimental

The experimental arrangement for the spectral response of the PEC cell is shown schematically in Fig. 10.1. The arrangement consists of a grating monochromator (HM 104, Central Electronics Limited (CEL)) and a PEC cell fabricated in our laboratory. The spectral response is observed for the wavelengths from 400 nm to 900 nm with an interval of 10 nm. A time interval of minimum two minutes was kept between two successive readings to avoid

the error due to the speed of response of the cell. The photocurrents were noted with the help of digital multimeter (Agronic-67).

Flat band potential measurements were carried out by using LCR meter (VLCR-23) with 1 KHz frequency. A saturated calomel reference electrode was used to measure the potential applied to semiconductor electrode. The impedance measurements were obtained while keeping the cell well protected from light. A diagram representing the experimental set up of PEC cell for capacitive measurements is same as given in Chapter 8 (Fig. 8.2).

10.3 Results and Discussion

10.3.1 Spectral response

The study of spectral response contains the information which is useful in identifying the recombination centres and consequently in diagnosing the problems which lead to the efficiency losses /1,2/. The short circuit photocurrent spectra of different photoactive materials have been reported by many workers /3,4-7/.

Fig. 10.2 shows the relative photocurrent spectra of the PEC cells which were fabricated by different electrodes of different compositions ($0 \leq x \leq 2$). A peak

has been noticed at a particular wave length in all the cases (Fig. 10.2). It is clear from Fig. 10.2 that photocurrent decreases on both, higher as well as the lower wavelength sides of the peak. At high energy photons, the absorption coefficient increases which may given rise to a large number of carriers. This in turn results in an enhanced recombination. Higher values of recombination velocity at surface cause a strong reduction of photocurrent with increasing photon energy. While for the low energy photons, the production of charge carriers decreases and one observes low photocurrent.

Moreover, it should be noted that the peak position is obtained at particular optimum wavelength. At this wavelength, maximum photocurrent is obtained which yields the direct band gaps of the semiconductors used in the Cell. The onset of the photocurrent also enables one to evaluate the direct band gap. This can be obtained by the simple equation

$$E_g = h\nu \qquad (10.1)$$

The direct band gaps determined with the help of above equation by employing peak values and onset values of wavelengths are given in Table 10.1.

The values from the present work are found to be in good agreement with those reported in the literature. The variation of band gap with composition is displayed in Fig. 10.3.

10.3.2 Flat band potential measurements

The energy levels in the electrolyte (redox potentials) are generally known as a function of electrolyte composition /8/ or can easily be determined. However, the energy levels in the semiconductor are more difficult to obtain. For semiconducting electrodes, the usual procedure is to measure some property which depends on applied potential and extrapolate to the flat band condition.

When the semiconductor electrode is immersed in the electrolyte, a junction is formed at the semiconductor/electrolyte interface which can be represented as two capacitances in series, one in the electrolyte near the surface (Helmholtz layer) C_H and another capacitor C_{sc} formed in the semiconductor by depletion region C_{sc} /9/. Since these two capacitors are in series and $C_{sc} \leq C_H$, the net capacitance is almost C_{sc} only.

The width of the depletion layer depends on the applied

potential. As the depletion layer width goes to zero at the flat band potential, the capacitance of the junction goes to infinity. An analysis of this type of behaviour for solid state devices has shown that $1/C^2$ varies linearly with applied potential which is nothing but the famous Mott-Schottky plot. This approach can be applied to the semiconductor/electrolyte junction /10/.

The Mott-Schottky plots of applied potential versus C^{-2} using the WS_xSe_{2-x} single crystal electrodes, are displayed in Fig. 10.4. These data were obtained from impedance measurements. These plots (Fig. 10.4) show good linearity over a limited range of potentials. The intercepts on the X-axis of these plots enabled us to estimate the flat band potentials. These values are given in Table 10.2. Gobrent et al /11/ have reported the values of flat band potentials for p-WSe_2 single crystals to be (0.8 ± 0.2) volt. Looking to this result, it is felt that present results (Table 10.2) are quite satisfactory. From the slope of the above Mott-Schottky plots, apparent values of N_A (acceptor density) were calculated (as shown in chapter 8) which are given in Table 10.2. The crystals described above were used with either no further pretreatment or after peeling the top layer from

the surface with adhesive tape.

Now in order to determine the energetic location of the valence and conduction band edges, the procedure /12/ outlined below for p-type electrodes is used.

The difference between E_V and E_F can be obtained from the equation

$$N_A = N_V \exp\left[E_V - E_F / kT\right] \qquad (10.2)$$

where N_A is the acceptor density (all acceptor impurities are assumed to be completely ionised), E_V is the energy at the edge of the valence band, E_F, the Fermi level energy and N_V, the density of effective states in the valence band. This last term is given by

$$N_V = 2\left(\frac{2\pi m_e^* kT}{h^2}\right)^{3/2} \qquad (10.3)$$

Taking the effective mass of the electron m_e^* as equal to that of the free electron (m_0) (which may introduce a significant error in calculating N_V), and assuming that the value for WS_xSe_{2-x} is similar to that for $MoSe_2$ /13/, the value

of N_V is estimated to be 2.6×10^{19} cm^{-3}. With this value and the experimental value for E_A, the difference between the edge of the valence band and Fermi level ($E_V - E_F$) is obtained. This places the edge of the valence band at particular value in volts Vs.SCE. By subtracting the band gap energy from this value, the location of the conduction bandedge (E_C) is placed at some volts. Thus the complete energy level diagram for the PEC cell is obtained and is shown in Fig. 10.5 for all the compositions. The results are supported by the reported values for p-MSe_2 in the literature /14/.

10.4 Conclusions

1. Spectral response of the photoelectrode of MS_xSe_{2-x} series gives uniform variation in band gap with composition.

2. A systematic variation in the flat band potential with compositions is also observed.

3. Energy level diagram obtained from the Mott-Schottky plots gives the complete idea about the semiconducting behaviour of the MS_xSe_{2-x} single crystals in the PEC solar cells.

Table 10.1

Energy band gap of WS_xSe_{2-x} single crystals

Crystal	Direct band gap (eV) present work		Direct band gap (eV) reported
	Onset value	Peak value	
WSe_2	1.46	1.63	1.60 /13/ 1.57 /15/
$WS_{0.5}Se_{1.5}$	1.50	1.72	-
WSSe	1.60	1.82	-
$WS_{1.5}Se_{0.5}$	1.71	1.85	-
WS_2	1.77	1.95	1.95 /3/ 1.78 /16/

Table 10.2

Flat band potentials (V_{fb}) and carrier concentration (N_A) for different compositions

Crystals	Flat band potentials (V_{fb}) in volts (Vs SCE)	Carrier concentration (N_A) / cm^3
WSe_2	0.75	4.043×10^{17}
$WS_{0.5}Se_{1.5}$	0.90	7.0449×10^{17}
$WSSe$	1.02	13.1068×10^{17}
$WS_{1.5}Se_{0.5}$	1.30	3.8941×10^{17}
WS_2	1.50	3.0264×10^{17}

References

/1/ Heller, A. (1977).
Semiconductor liquid junction solar cells.
(The electrochemical society, Princeton, New Jersey).

/2/ Heller, A., Chang, K. C., and Miller, B. (1977).
J. Electrochem. Soc. 124 , 697.

/3/ Tributsch, H. (1977).
Ber. Bunsenges. Phys. Chem. 81 , 361.

/4/ Hardee, K. L. and Bard, A. J. (1975).
J. Electrochem. Soc. 122 , 739.

/5/ Mavroides, J. G., Tchernev, D. I., Kafalas, J. A. and Kolesar, D. (1975).
Mat. Res. Bull. 10 , 1023.

/6/ Wrighton, M. S., Ellis, A. B., Wolczanski, P. T., Morse, D. L., Abrahamson, A. B. and Ginley, D. S. (1976).
J. Am. Chem. Soc. 98 , 2274.

/7/ Mavroides, J. G., Kafalas, J. and Kolesar, D. (1976).
Appl. Phys. Lett. 28 , 241.

/8/ Dotson, D. (1975).
"Electrochemical Data"
(Elsevier, New York).

/9/ Vijh, A. K. (1975).
"Electrochemistry of Metals and Semiconductors"
(Dekker, New York).

/10/ Eyring, H., Henderson, D. and Jost, W. (Ed.)(1970).
"Physical Chemistry : An advance treatise,
Vol. 9A (Academic Press).

/11/ Gobrecht, J., Gerischer, H. and Tributsch, H. (1978). Ber. Bunsenges. Phys. Chem. 82, 1331.

/12/ Abruna, H. D., Hope, G. A. and Bard, A. J. (1982). J. Electrochem. Soc. 129, No. 10, 2224.

/13/ Hiehm, W. T. (1964). J. Electrochem. Soc. 111, 1058.

/14/ Nagasubramanian, G. and Bard, A. J. (1981). J. Electrochem. Soc. 128, No. 5, 1055.

/15/ Upadhyayula, L. C., Loferski, J. J., Wold, A., Giriat, W. and Kershaw, R. (1968). J. Appl. Phys. 39, 4736.

/16/ Baglio, J. A., Calabrese, G. S., Kamieniecki, E., Kershaw, R., Kubiak, C. P., Ricco, A. J., Wold, A., Wrighton, M. S. and Zoski, G. D. (1982). J. Electrochem. Soc. 129, 1461.

Captions to the Figures

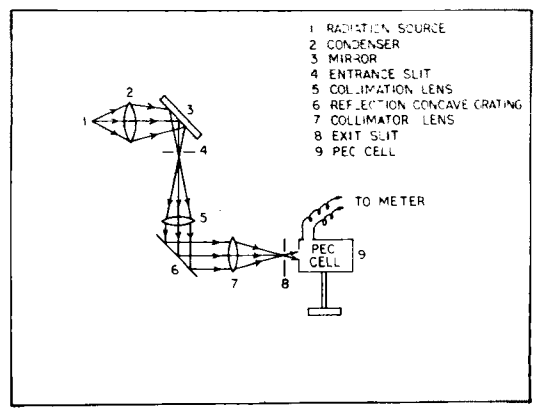

Fig. 10.1

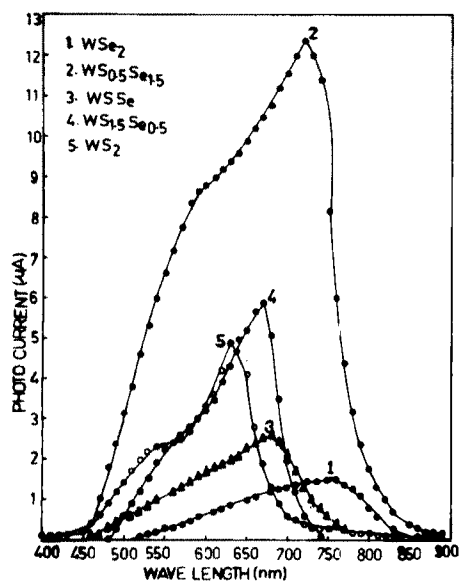

Fig. 10.2

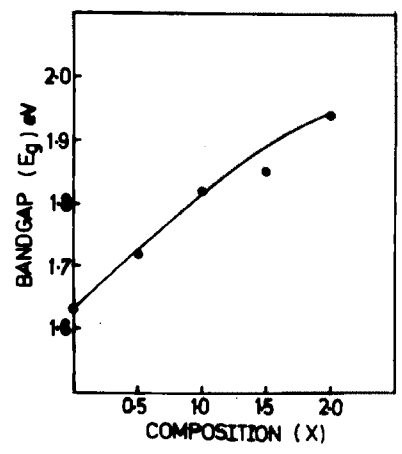

Fig. 10.3

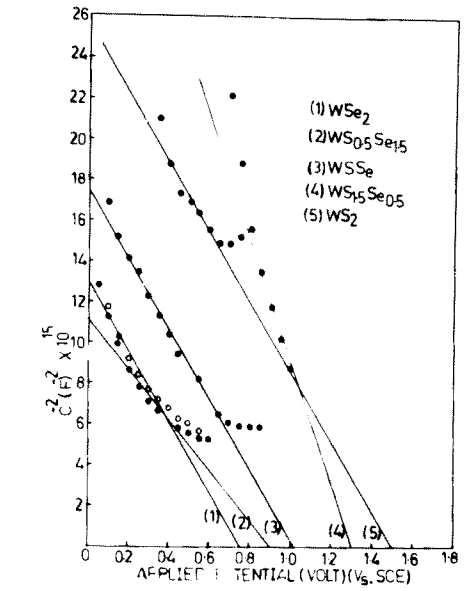

Fig. 10.4

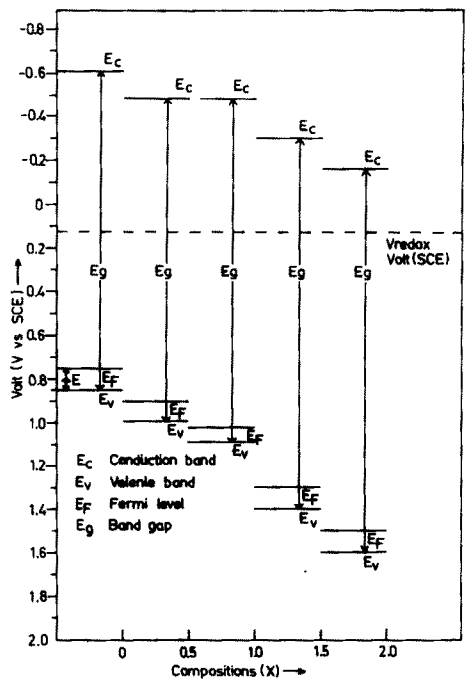

Fig. 10.5